Electronic Supplementary Information

Organometallo-macrocycle assembled through dialumane-mediated C–H activation of pyridines

Weixing Chen,[#a] Li Liu,[#a] Yanxia Zhao,*[a] Yujie Xue,[a] Wenhua Xu,[a] Nan Li,*[b] Biao Wu[a,c] and Xiao-Juan Yang*[a,c]

[a] *Key Laboratory of Synthetic and Natural Functional Molecule Chemistry of the Ministry of Education College of Chemistry and Materials Science, Northwest University Xi'an 710069, China*

[b] *State Key Laboratory of Explosion Science and Technology, School of Mechatronical Engineering, Beijing Institute of Technology, Beijing 100081, China.*

[c] *Key Laboratory of Medical Molecule Science and Pharmaceutics Engineering, Ministry of Industry and Information Technology, School of Chemistry and Chemical Engineering, Beijing Institute of Technology, Beijing 100081, China*

[#]*W. Chen and L. Liu contributed equally to this work.*

**Correspondence: zhaoyx@nwu.edu.cn; leen04@bit.edu.cn; yangxiaojuan@nwu.edu.cn*

Table of Contents

S1. Experimental Details

General Procedures

All of the reactions and manipulations of air- and moisture-sensitive compounds were carried out under argon or nitrogen with standard Schlenk or drybox techniques. The solvents (toluene, THF, Et_2O and DME) were dried using appropriate methods and were distilled under argon prior to use. Benzene-d_6 and THF-d_8 were dried over Na/K alloy. The α-diimine ligand L was prepared according to literature procedures.[1] Sodium metal, anhydrous aluminum chloride ($AlCl_3$), pyridine (Py), 4-picoline, 3-picoline, and 2-picoline were purchased from Alfa Aesar. NMR spectra were recorded on a Mercury Plus-400 spectrometer. Elemental analyses were performed with an Elementar VarioEL III instrument. EPR spectra were recorded on a Bruker E500-9.5/12 spectrometer at room temperature by using a standard resonance cavity. IR spectra were recorded using a Nicolet AVATAR 360 FT-IR spectrometer.

Synthesis

Synthesis of [L(Py)Al–Al(Py)L] (2)

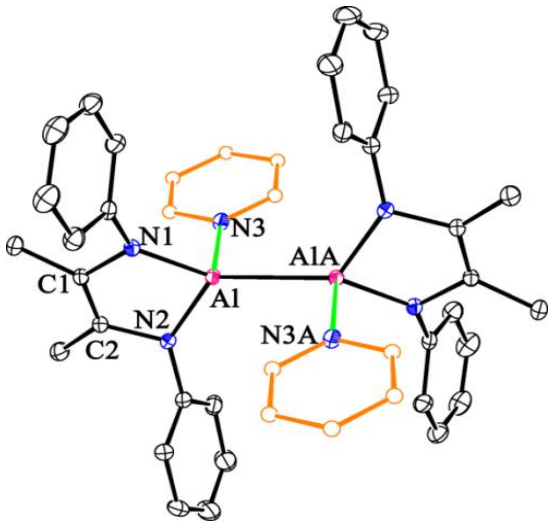

Fig. S1. Molecular structure of **2** (thermal ellipsoids are set at the 20% probability level; H atoms and iPr groups of ligand L are omitted for clarity). Selected bond lengths (Å) and angles (°): Al–AlA 2.685(2), Al–N1 1.863(3), Al–N2 1.866(3), Al–N3 2.060(3), C1–N1 1.432(4), C2–N2 1.440(4), C1–C2 1.348(5), N1–Al–N2 89.50(13), N1–Al–AlA 127.83(11), N2–Al–AlA 128.14(11). Symmetry code: (A) 1–*x*, 1–*y*, 1–*z*.

Pyridine (2.0 mmol) was slowly added to a solution of precursor [L(THF)Al−Al(THF)L] (**1**)[2] (1.0 mmol) in 30 mL of toluene, and the color changed from deep-red to brown. The mixture was stirred at room temperature for 1 day and then filtered, and the filtrate was concentrated to about 5 mL. Dark red crystals (0.940 g, 92%) of complex **2** were grown by slow evaporation of the toluene solution. ^{1}H NMR (400 MHz, C_6D_6): δ = 0.80 (br, 12H; CH(CH_3)$_2$), 1.18 (br, 12H; CH(CH_3)$_2$), 1.64 (s, 6H; CCH_3), 3.34 (br,

4H; C*H*(CH_3)$_2$), 6.43 (br, 2H; Py), 6.78 (br, 1H; Py), 7.07−7.12(m, 6H; Ar), 8.48 (br, 2H; Py). ^{13}C NMR (101 MHz, THF-d_8): δ = 15.4 (N−C*C*H_3), 24.8 (CH(*C*H_3)$_2$), 25.0 (CH(*C*H_3)$_2$), 28.0 (*C*H(CH_3)$_2$), 119.6 (N−*C*CH_3), 123.4, 123.5 (Py), 124.2, 124.3 (Py), 135.2 (Py), 136.6, 147.9 (Ar), 150.3 (Py). IR (Nujol, cm^{-1}): 2922 s, 2855 s, 1609 m, 1460 s, 1377 s, 1313 m, 1246 m, 1207 w, 1170 w, 937 w, 787 m, 725 m, 696 w, 638 w, 430 m. Elemental analysis calcd. for $C_{66}H_{90}Al_2N_6$ (1021.45): C 77.61, H 8.88, N 8.23. Found: C 78.09, H 8.89, N 8.00%.

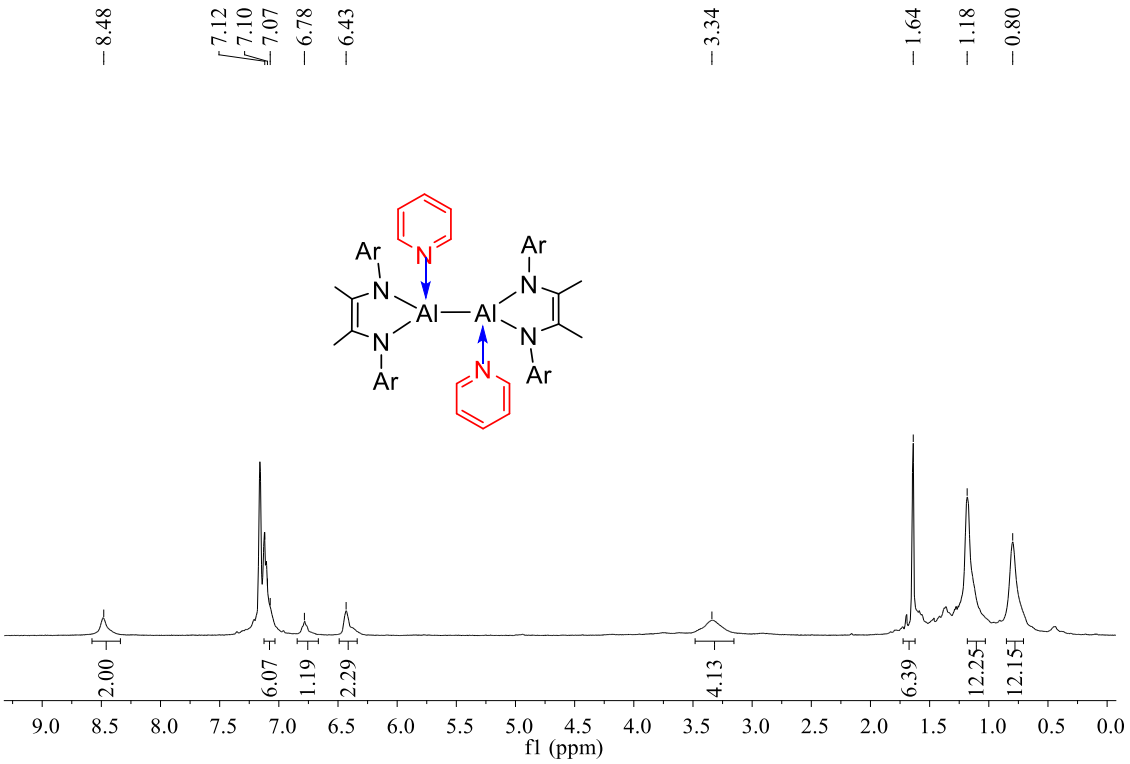

Fig. S2. ^{1}H NMR spectrum of **2** in C_6D_6.

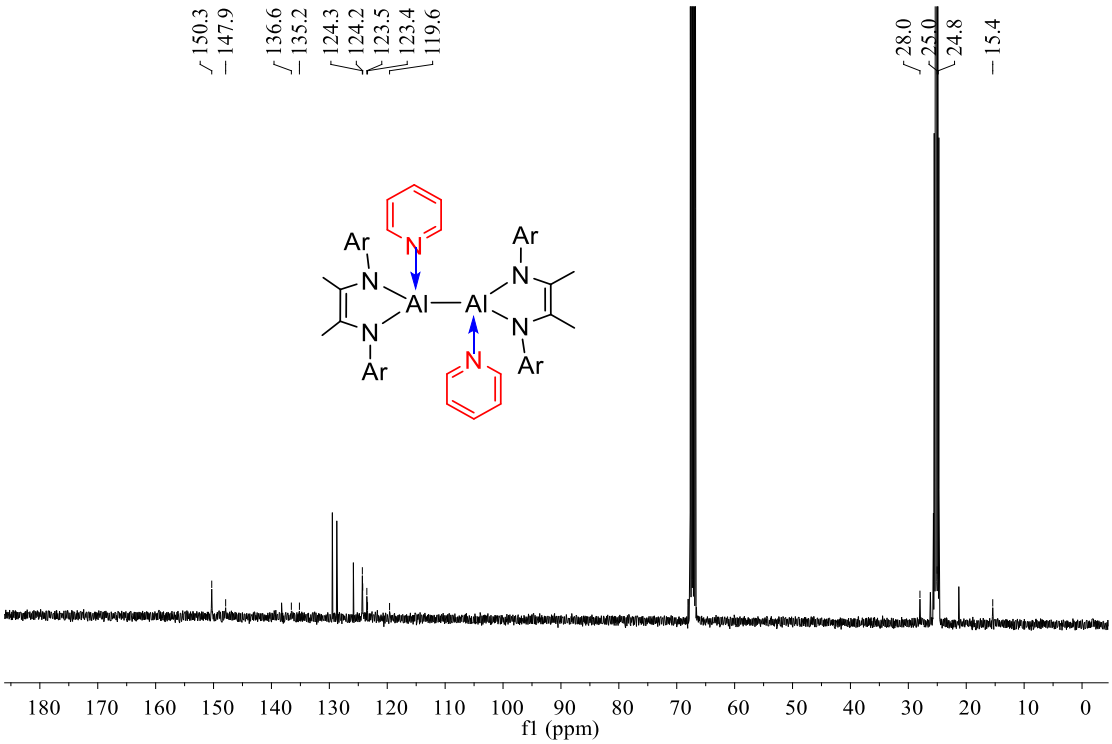

Fig. S3. ^{13}C NMR spectrum of **2** in THF-d_8.

Synthesis of [{LAl(pyridyl)}$_6$] (3)

Compound **2** (160 mg, 0.157 mmol) was dissolved in 10 mL toluene in a sealed tube, and the solution was stirred at 80 ℃ for 24 hours. The color of the solution changed from brown to dark blue. The reaction mixture was filtered and the filtrate was concentrated to about 5 mL. Blue crystals were grown at −20 °C (0.120 g, 75%). ^{1}H NMR (400 MHz, THF-d_8): δ = –0.17 (d, 3H; CH(CH_3)$_2$), 0.41 (d, 3H; CH(CH_3)$_2$), 0.82 (d, 3H; CH(CH_3)$_2$), 0.89 (d, 3H; CH(CH_3)$_2$), 1.01 (d, 3H; CH(CH_3)$_2$), 1.09 (d, 3H; CH(CH_3)$_2$), 1.22 (br, 6H; CH(CH_3)$_2$), 1.53 (s, 6H; CCH_3), 3.10 (m, 1H; CH(CH$_3$)$_2$), 3.40 (m, 1H; CH(CH$_3$)$_2$), 3.51 (m, 2H; CH(CH$_3$)$_2$), 6.78–7.13 (m, 6H; Ar), 7.19 (d, 1H; Py), 7.38 (m, 1H; Py), 7.51(s, 1H; Py), 8.78 (s, 1H; Py). ^{13}C NMR (101 MHz, THF-d_8) δ = 14.1 (N−CCH$_3$), 14.3 (N−CCH$_3$), 16.4 (N−CCH$_3$), 18.4 (N−CCH$_3$), 19.1 (N−CCH$_3$), 22.7 (CH(CH_3)$_2$), 23.0 (CH(CH_3)$_2$), 23.2 (CH(CH_3)$_2$), 23.6 (CH(CH_3)$_2$), 24.0 (CH(CH_3)$_2$), 24.3 (CH(CH_3)$_2$), 25.9 (CH(CH_3)$_2$), 26.0 (CH(CH_3)$_2$), 27.5 (CH(CH_3)$_2$), 27.8 (CH(CH_3)$_2$), 28.1 (CH(CH$_3$)$_2$), 28.2 (CH(CH$_3$)$_2$), 28.6 (CH(CH$_3$)$_2$), 29.2 (CH(CH$_3$)$_2$), 120.0 (N−CCH$_3$), 121.1 (N−CCH$_3$), 123.1, 123.3, 123.8, 124.0 (Py), 124.4, 124.7, 125.0, 135.4 (Py), 136.6 (Py), 142.3, 142.8, 143.8, 144.0, 146.9, 147.4, 147.5 (Ar), 148.3 (Py), 148.5 (Py). IR (Nujol, cm^{-1}): 2922 s, 2855 s, 1605 w, 1460 s, 1377 s, 1253 w, 1153 w, 1211 w, 723 m. Elemental analysis calcd. for $C_{198}H_{264}Al_6N_{18}$ (3058.31): C 77.76, H 8.70, N 8.24. Found: C 78.25, H 8.75, N 7.75%.

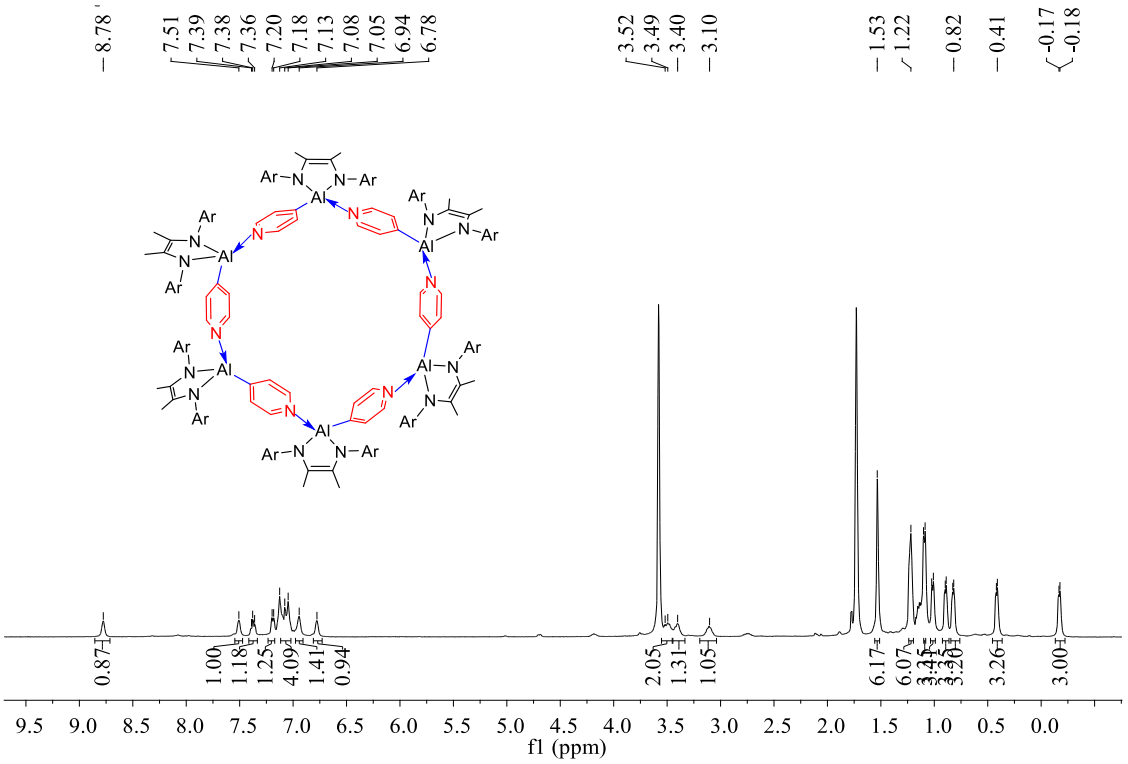

Fig. S4. ^{1}H NMR spectrum of **3** in THF-d_8.

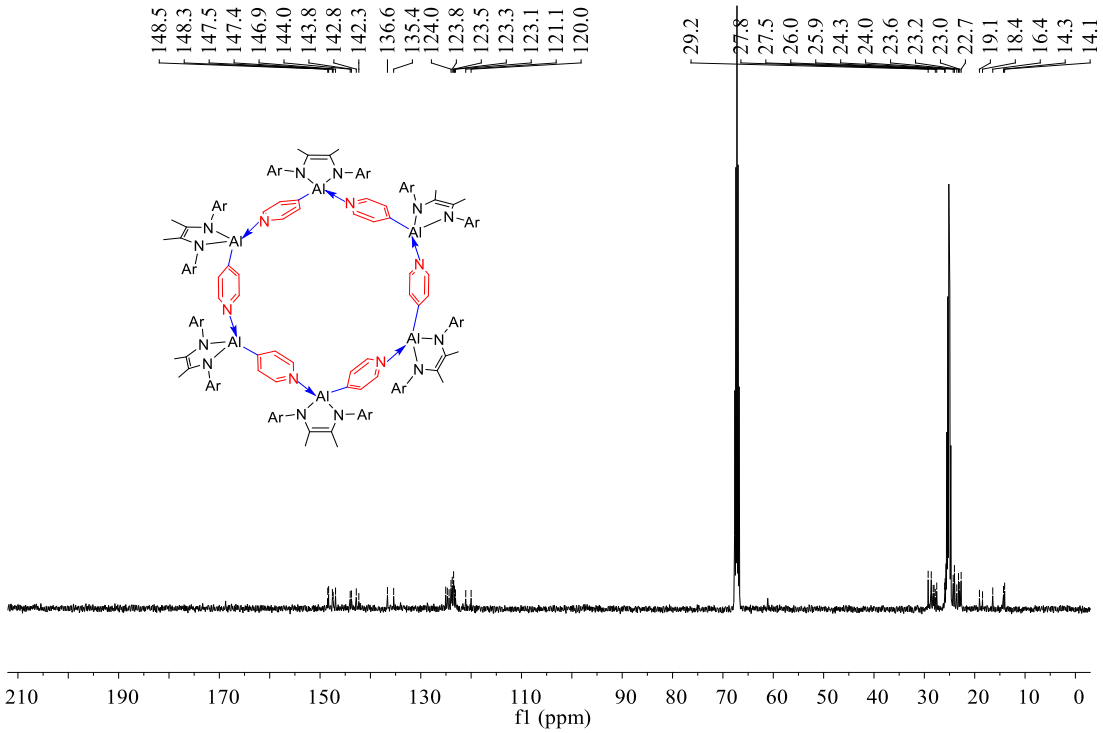

Fig. S5. ^{13}C NMR spectrum of **3** in THF-d_8.

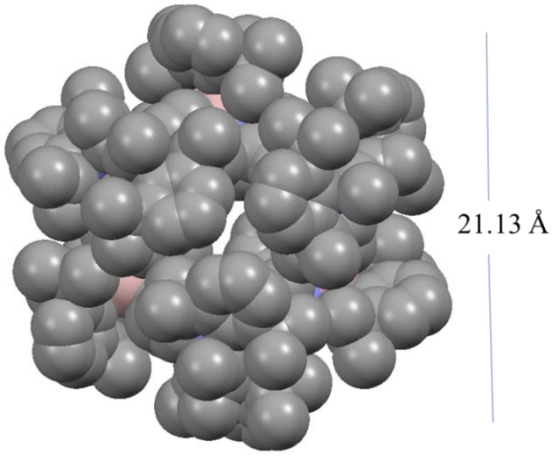

Fig. S6. Space filling model of complex **3** showing its size.

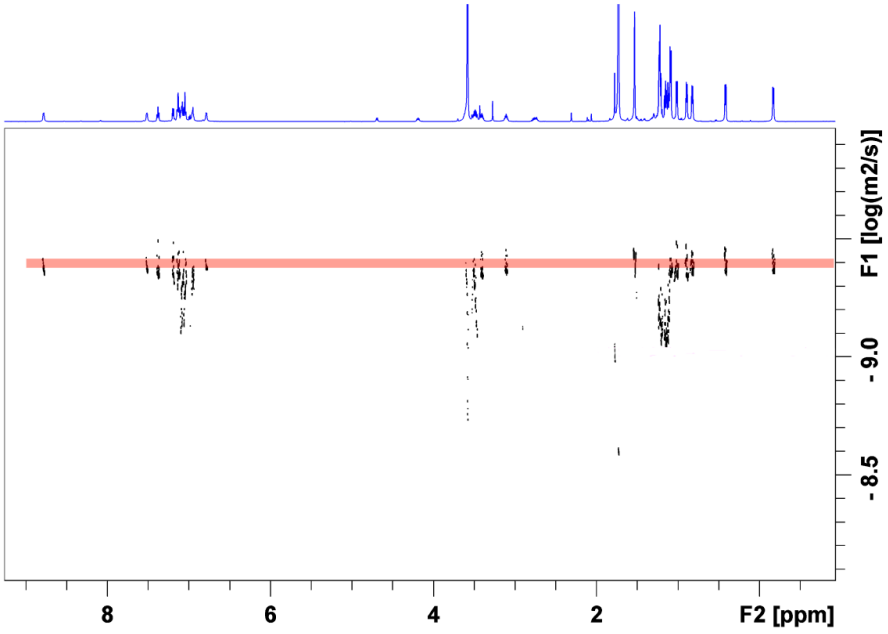

Fig. S7. DOSY spectrum (400 MHz, THF-d_8, 298 K, log D = −9.40) of **3**.

Diffusion coefficients and hydrodynamic radii are correlated theoretically by the Stokes-Einstein Relation (**Equation S1**): $r = \frac{kT}{6\pi\eta D}$ where D is the diffusion coefficient ($10^{-9.40}$ = 3.98×10^{-10} obtained from Fig. S7), k is the Boltzmann constant 1.38×10^{-23} m^2 kg s^{-2} K^{-1}), T is the temperature in Kelvin (298 K), η is the viscosity of the solvent (THF 5.01×10^{-4} kg m^{-1} s^{-1})[3], and r is the radius of the molecular sphere.

$$r(\mathbf{3}) = 1.38\times10^{-23}\times298/(6\times3.14\times5.01\times10^{-4}\times3.98\times10^{-10})=1.09\times10^{9}\ \text{m} = 10.9\ \text{Å}$$

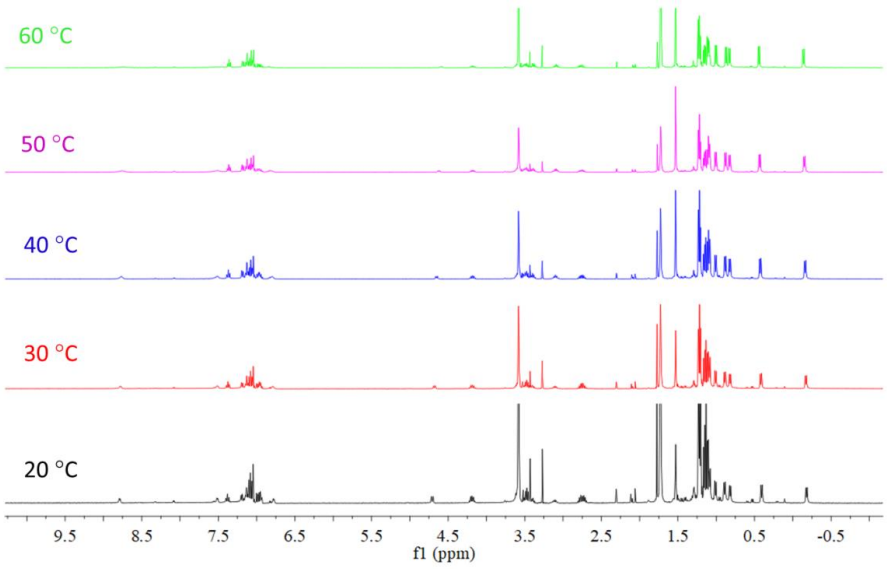

Fig. S8. Variable-temperature ^{1}H NMR spectra of compound **3** (THF-d_8, 400 MHz).

Synthesis of [L(4-picoline)Al–Al(4-picoline)L] (4a), [L(3-picoline)Al–Al(3-picoline)L] (4b) and [L(2-picoline)Al–AlL] (4c).

In a similar procedure to that for compound **2**, 4-picoline, 3-picoline, or 2-picoline (2.0 mmol) was slowly added to a solution of dialumane **1** (1.0 mmol) in 30 mL of toluene, and the mixture was stirred at room temperature for 1 day, upon which the color changed from deep-red to brown. The reaction mixture was filtered and the filtrate was concentrated to about 5 mL. Dark red crystals of **4a**−**4c** were crystallized by slow evaporation of the toluene solution for several days.

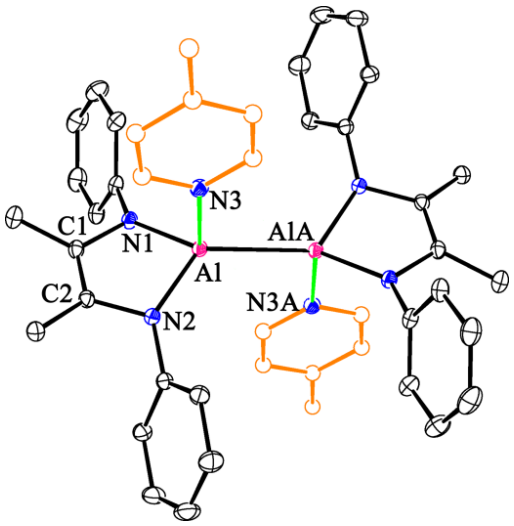

Fig. S9. Molecular structure of **4a** (thermal ellipsoids are set at the 20% probability level; H atoms and *i*Pr groups of L are omitted for clarity). Selected bond lengths (Å) and angles (°): Al–AlA 2.6789(9), Al–N1 1.8663(13), Al–N2 1.8631(12), Al–N3 2.0612(13), C1–N1 1.4300(18), C2–N2 1.4293(18), C1–C2 1.342(2), N1–Al–N2 89.28(5), N1–Al–N3 99.76(5), N3–Al–AlA 106.18(4), N1–Al–AlA 127.57(4), N2–Al–AlA 128.13(5). Symmetry code: (A) 1-*x*, 1-*y*, 1-*z*.

Complex 4a•toluene (0.98 g, 86%)**:** ^{1}H NMR (400 MHz, C_6D_6): δ = 0.82 (br, 12H; CH(CH_3)$_2$), 1.20 (br, 12H; CH(CH_3)$_2$), 1.62 (s, 3H; 4-picoline), 1.68 (s, 6H; CCH_3), 2.12 (toluene), 3.38 (m, 4H; CH(CH$_3$)$_2$), 6.34 (br, 2H; 4-picoline), 7.01−7.14 (toluene), 7.14−7.23(m, 6H; Ar), 8.49 (br, 2H; 4-picoline). ^{13}C NMR (101 MHz, C_6D_6): δ = 15.6 (N−CCH_3), 20.8 (4-picoline), 21.5 (toluene), 24.8 (CH(CH_3)$_2$), 25.8 (CH(CH_3)$_2$), 28.1 (CH(CH$_3$)$_2$), 121.8 (N−CCH_3), 123.5 (4-picoline), 124.4, 125.3 (4-picoline), 125.7 (toluene), 127.9 (4-picoline), 128.2, 128.6 (toluene), 129.3 (toluene), 137.9 (toluene), 146.7 (Ar), 147.7 (4-picoline). IR (Nujol, cm^{-1}): 2947 s, 2855 s, 1622 m, 1460 s, 1377 s, 1315 w, 1244 m, 1209 w, 1171 w, 1204 w, 937 w, 813 w, 785 m, 725 s, 569 w, 544 s, 494 w, 428 m. Elemental analysis calcd. for $C_{68}H_{94}Al_2N_6$·toluene ($C_{75}H_{102}Al_2N_6$ 1141.58): C 78.91, H 9.01, N 7.36. Found: C 78.42, H 9.15, N 7.74%.

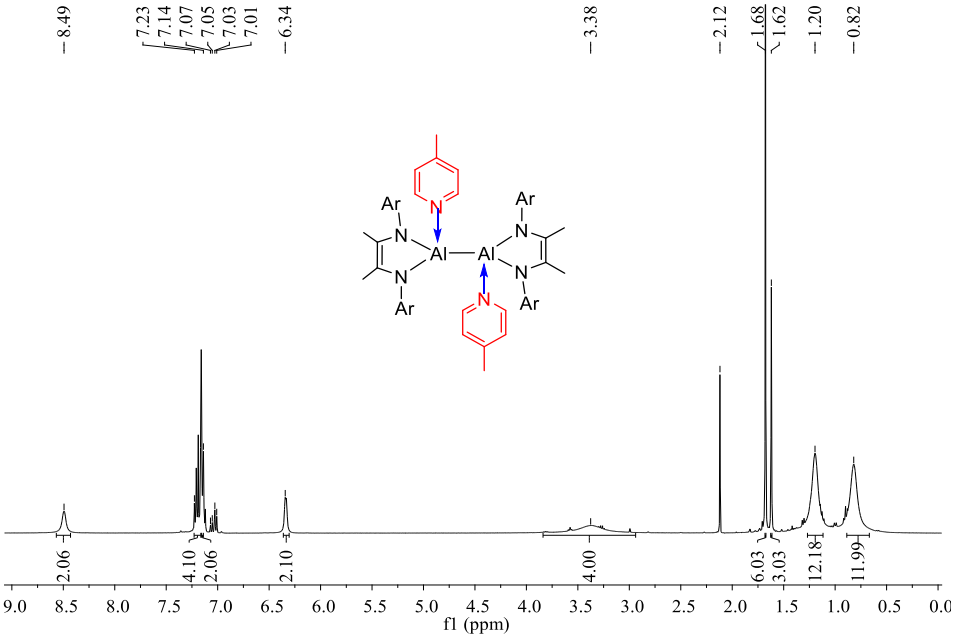

Fig. S10. ^{1}H NMR spectrum of **4a** in C_6D_6.

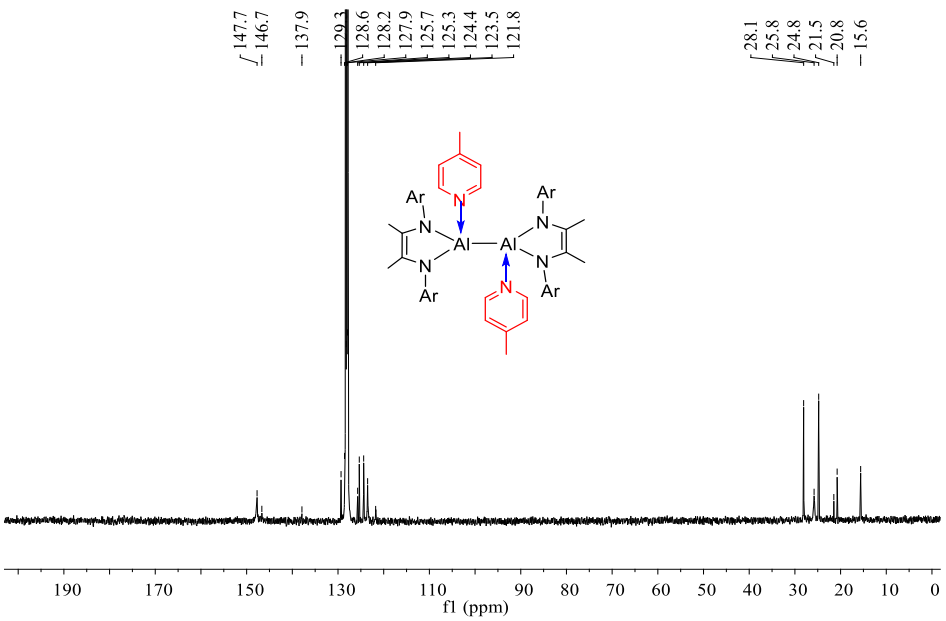

Fig. S11. ^{13}C NMR spectrum of **4a** in C_6D_6.

Complex 4b (1.068 g, 93%)**:** ^{1}H NMR (400 MHz, C_6D_6): δ = 0.85 (br, 12H; CH(C*H*$_3$)$_2$), 1.12 (Et_2O), 1.20 (br, 12H; CH(C*H*$_3$)$_2$), 1.64 (s, 6H; CC*H*$_3$), 1.70 (s, 3H; 3-picoline), 3.28 (Et_2O), 3.41 (m, 4H; C*H*(CH$_3$)$_2$), 6.41 (br, 1H; 3-picoline), 6.68 (br, 1H; 3-picoline), 7.12−7.18(m, 6H; Ar), 8.08 (br, 1H; 3-picoline), 8.45(br, 1H; 3-picoline). IR (Nujol, cm^{-1}): 2924 s, 2854 s, 1612 m, 1460 m, 1377 s, 1315 s, 1244 m, 1207 w, 1173 w, 1120 w, 1063 w, 937 w, 985 m, 723 m, 658 w. Elemental analysis calcd. for $C_{68}H_{94}Al_2N_6$ (1149.45): C 77.82, H 9.03, N 8.01. Found: C 77.93, H 9.01 N, 7.75%.

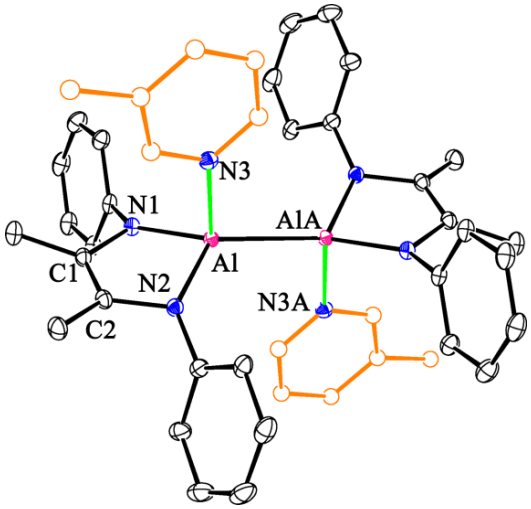

Fig. S12. Molecular structure of **4b** (thermal ellipsoids are set at the 20% probability level; H atoms and *i*Pr groups of L are omitted for clarity). Selected bond lengths (Å) and angles (°): Al–AlA 2.6677(8), Al–N1 1.8616(12), Al–N2 1.8676(12), Al–N3 2.0675(12), C1–N1 1.4338(18), C2–N2 1.4353(18), C1–C2 1.345(2), N1–Al–N2 89.97(5), N1–Al–N3 98.96(5), N3–Al–AlA 107.15(4), N1–Al–AlA 128.34(4), N2–Al–AlA 126.62(4). Symmetry code: (A) 1-*x*, 1-*y*, 1-*z*.

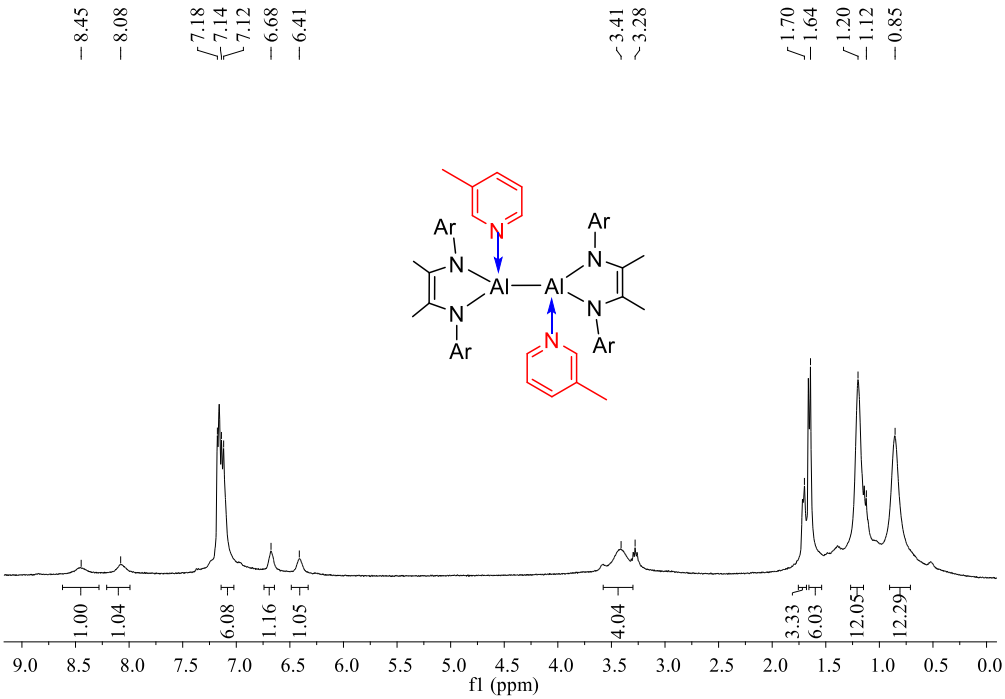

Fig. S13. ^{1}H NMR spectrum of **4b** in C_6D_6.

Complex 4c•toluene (0.655 g, 57%)**:** IR (Nujol, cm^{-1}): 2955 s, 2855 s, 1643 m, 1460 s, 1377 s, 986 s, 727 s, 694 m, 496 s. Elemental analysis calcd. for $C_{62}H_{87}Al_2N_5$·toluene (1148.52): C 79.04, H 9.13, N 6.68. Found: C 78.55, H 9.02, N 7.03%. EPR (THF, 295 K): frequency 9.826 GHz, g = 2.000.

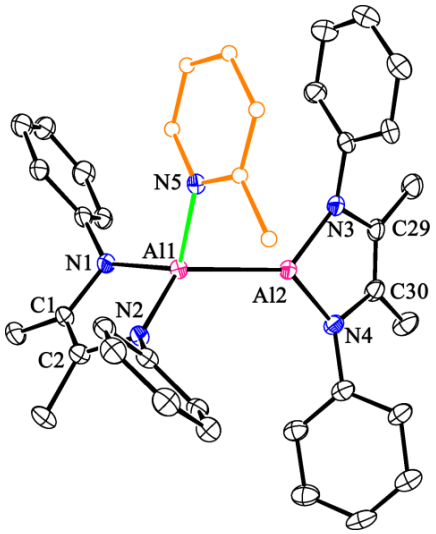

Fig. S14. Molecular structure of **4c** (thermal ellipsoids are set at the 20% probability level; H atoms and *i*Pr groups of L are omitted for clarity). Selected bond lengths (Å) and angles (°): Al1–Al2 2.6043(15), Al1–N1 1.848(3), Al1–N2 1.843(3), Al1–N5 2.027(3), Al2–N3 1.823(3), Al2–N4 1.819(3), C1–N1 1.434(5), C2–N2 1.444(5), C1–C2 1.336(5), N3–C29 1.427(5), N4–C30 1.436(5), C29–C30 1.338(6), N1–Al1–N2 117.60(12), N1–Al1–N5 112.10(14), N2–Al1–N5 114.00(14), N5–Al1–Al2 95.29(10), N3–Al2–N4 90.00(15).

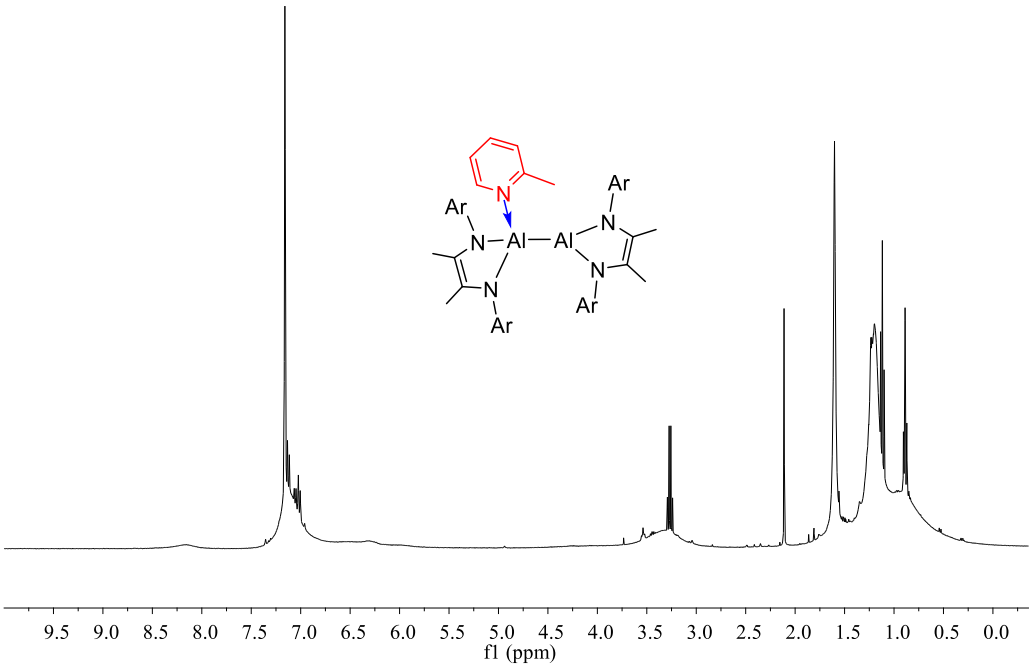

Fig. S15. ^{1}H NMR spectrum of **4c** in C_6D_6.

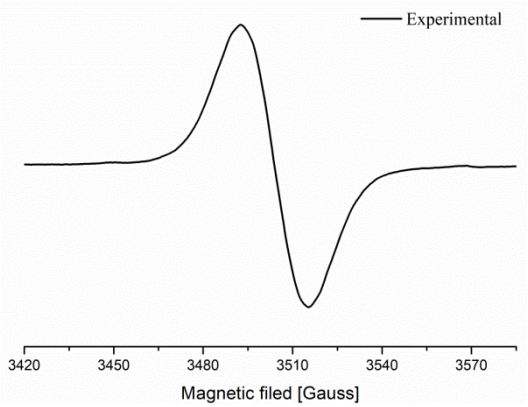

Fig. S16. X-band EPR spectrum of **4c** in THF at room temperature. Experimental conditions: frequency = 9.826 GHz (g = 2.000).

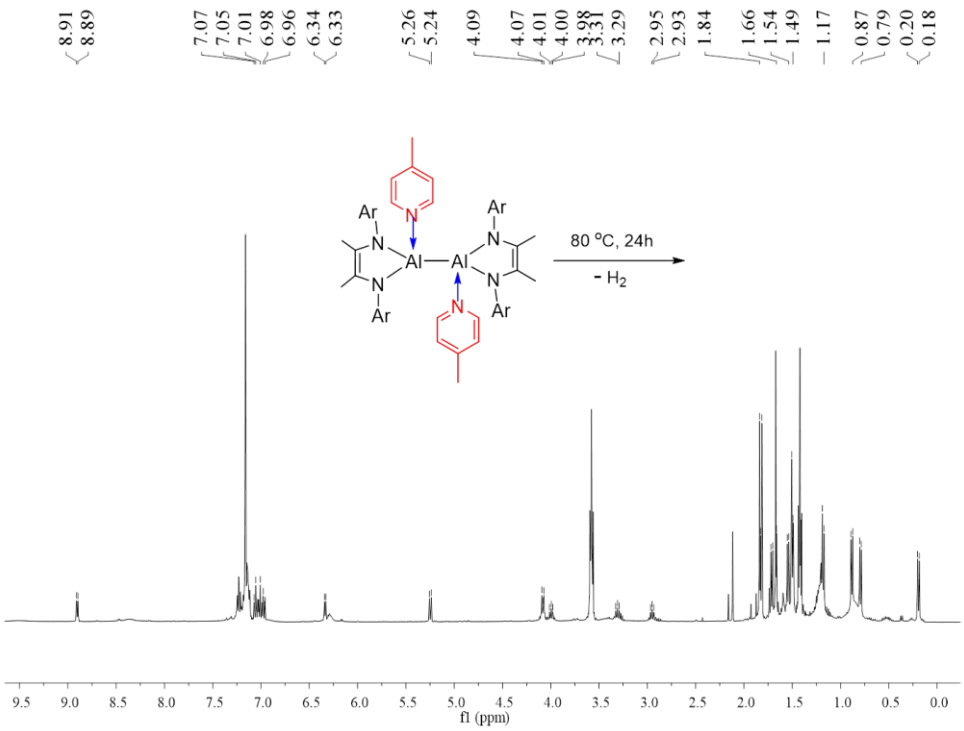

Fig. S17. ^{1}H NMR monitoring reveals changes after heating **4a** for 12 hours at 80 ℃ in C_6D_6.

S2. X-ray Crystallographic Analysis

Diffraction data for complexes **2**, **3** and **4a**–**4c** were collected on a Bruker SMART APEX II diffractometer at 150 K (for **2**, **3**, **4b** and **4c**), 159 K (for **4a**) with graphite-monochromated Mo Kα radiation (λ = 0.71073 Å). An empirical absorption correction using SADABS was applied for all data.[4] The structures were solved and refined to convergence on F^2 for all independent reflections by the full-matrix least squares method using the SHELXL−2014 programs[5] and OLEX2 1.2.[6]

In compound **3**, about 7 molecules of toluene (about 7 toluene molecules per formula, Z = 1) are co-crystallized, with the corresponding electron density (364 electrons) being removed. In compound **4c**, about 4 molecules of toluene (about 1 toluene molecules per formula, Z = 4) are co-crystallized, with the corresponding electron density (204 electrons) being removed., using the SQUEEZE routine implemented within the software program PLATON,[7] and the resulting .fab file was processed with OLEX2 1.2 using the ABIN instruction. Crystallographic data and refinement details for compounds **2**, **3** and **4a–4c** are given in Table S1–S3. CCDC numbers 2020863 (for **2**), 2020867 (for **3**), 2020864 (for **4a**), 2020865 (for **4b**), 2020866 (for **4c**). These data can be obtained free of charge from the Cambridge Crystallographic Data Centre www.ccdc.cam.ac.uk/data_request/cif.

Molecules of complexes **4a** and **4b** possess crystallographically imposed inversion centers in the center of the line that connects the metal atoms. The Al atoms in **4a** and **4b** exhibit distorted tetrahedral geometry with considerably longer Al–$N_{dpp\text{-}dad}$ distances (1.8616(12)–1.8676(12) Å) for the four-coordinate Al atom than those in **4c** (1.848(3) and 1.843(3) Å), and these bonds are much longer than those of the three-coordinate Al center (Al2, 1.823(3) and 1.819(3) Å) in **4c**. Besides, the dative Al–N_{py} (2.027(3)–2.0675(12) Å) bonds are markedly longer than the above covalent Al–$N_{diimine}$ bonds. The

observed Al–Al bond lengths in **4a** and **4b** (2.6789(9)–2.6677(8) Å) are close to that in **1** (2.658(2) Å) and **2** (2.684(2) Å) but are longer than that in **4c** (2.604(2) Å).

Table S1. Crystallographic data and refinement details for compounds **2** and **3**.

Compound	**2**	**3**
Empirical formula	$C_{66}H_{90}Al_2N_6$·toluene	$C_{198}H_{264}Al_6N_{18}$·7toluene
Fw	1113.53	3703.29
Crystal system	Monoclinic	Triclinic
Space group	$P2_1/n$	$P\bar{1}$
a /Å	12.469(8)	17.0990(17)
b /Å	13.297(8)	18.593(2)
c /Å	19.852(13)	21.710(2)
α / °	90	110.622(3)
β / °	97.499(19)	112.963(3)
γ / °	90	90.689(3)
V /Å^3	3263(4)	5857.9(10)
Z	2	1
D_{calc}/g cm^{-3}	1.133	0.867
F (000)	1208	1656
μ /mm^{-1}	0.090	0.071
Reflns collected	21065	74989
Independent reflns	6160	21315
Reflns [$I > 2\sigma(I)$]	4857	10198
R_{int}	0.0361	0.1187
R_1; wR_2 [$I > 2\sigma(I)$]	0.0988; 0.2331	0.0827; 0.1623
R_1; wR_2 (all data)	0.1177; 0.2470	0.1689; 0.1919
GOF (F^2)	1.194	1.033

Table S2. Crystallographic data and refinement details for compounds **4a**–**4c**.

Compound	**4a**	**4b**	**4c**
Empirical formula	$C_{68}H_{94}Al_2N_6$·toluene	$C_{68}H_{94}Al_2N_6$	$C_{62}H_{87}Al_2N_5$· toluene
w	1141.58	1049.45	1048.52
Crystal system	Monoclinic	Monoclinic	Orthorhombic
Space group	$P2_1/n$	$P2_1/n$	$P2_12_12_1$
a /Å	14.224(3)	13.5982(6)	12.9942(4)
b /Å	11.946(2)	15.1449(7)	21.2069(6)
c /Å	19.650(4)	14.8412(7)	22.7887(7)
α / °	90	90	90
β / °	92.092(7)	92.994(2)	90
γ / °	90	90	90

V /Å^3	3336.6(12)	3052.3(2)	6279.8(3)
Z	2	2	4
D_{calc}/g cm^{-3}	1.136	1.142	1.012
F (000)	1240	1140	2080
μ /mm^{-1}	0.090	0.093	0.084
Reflns collected	24912	60957	35498
Independent reflns	6130	5591	11053
Reflns [$I > 2\sigma(I)$]	5463	4914	8468
R_{int}	0.0284	0.0571	0.0440
R_1; wR_2 [$I > 2\sigma(I)$]	0.0408; 0.0859	0.0415; 0.1402	0.0519; 0.0892
R_1; wR_2 (all data)	0.0456; 0.0884	0.0478; 0.1483	0.0748; 0.0979
GOF (F^2)	1.070	1.130	1.108

S3. Theoretical Calculations

DFT calculations were carried out at the B3LYP/6-31g*[8,9] level of theory for slightly simplified model compounds **2H**, **3H** and **4aH**–**4cH**, where the dpp groups were replaced by Ph, using the Gaussian 09 program.[10] Figures S18 shows the optimized geometries, which reproduce the experimental data of **2**, **3** and **4a**–**4c** reasonably well. The atomic populations, bonding orbitals and Wiberg bond orders were obtained with NBO method.[11-13] In the simple coordination adducts (**2H** and **4aH**–**4cH**), the Al–Al bond now displays the bond order of av. 0.93, which are same with that in the precursor **1H** (0.93). In the C–H activation of pyridine product **3H**, the bonds of Al–C display bond orders of av. 0.49, and the Al–$N_{pyridyl}$ bond order is av. 0.31, which is much larger than Al–$N_{pyridine}$ in **2H** and **4aH–4cH** (av. 0.22). Natural population analysis (NPA) suggests that the charge on Al (av. 1.79) in **3H** is much larger than that in precursor **1H** (1.13)[2] and **2H**, **4aH–4cH** (av.1.30), which displays a formal oxidation state of +3. The pyridyl unit in **3H** accumulates negative partial charges of –0.50 e, thus indicating the reduction of the neutral pyridine ligand in **2** (0.13 e) into the monoanion in **3**.

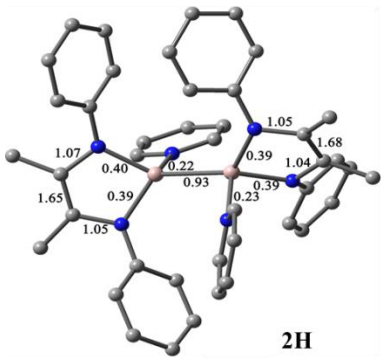

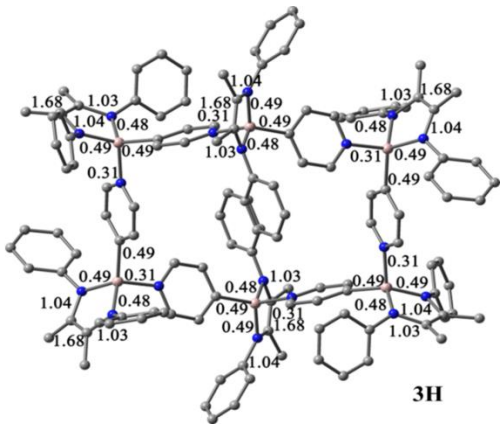

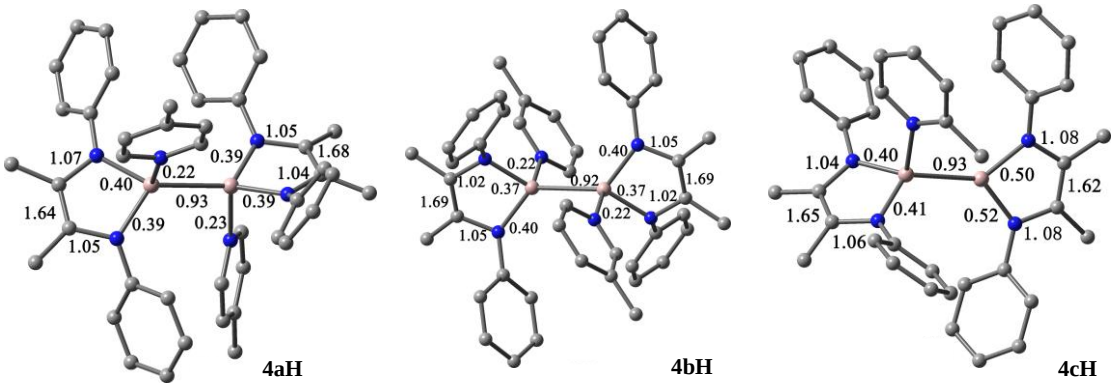

Fig. S18. Optimized structures of **2H, 3H and 4aH–4cH** labelled with selected bond orders.

Table S3. Natural charges (e) of the model compounds **2H, 3H** and **4aH**–**4cH**.

Compound	**2H**	**3H**	**4aH**	**4bH**	**4cH**
Al	1.32	1.79	1.32	1.34	1.34, 1.17
L	−1.43	−1.29	−1.44	−1.46	−1.41, −1.25
Small molecule (Py')	0.13	−0.50	0.13	0.12	0.14

Mechanism studies

DFT calculations (B3LYP/6-31G*) were carried out to determine a possible reaction pathway for the formation of **3** (Figs. S19, S20). Solvation effects and dispersion correction were included by performing single-point energy calculations.

The reaction begins with the homolytic Al–Al bond breaking of **2** to form a radical species [L(Py)Al•], which is similar to the homolytic B–B bond cleavage with 4-cyanopyridine.[15] Dissociation of **2** into two radicals costs 17.8 kcal mol^{-1} (ΔG) energy, which is somewhat easier than the dissociation energy of [L(THF)Al–Al(THF)L] into [L(THF)Al•] (ΔG = 19.8 kcal mol^{-1}), indicating that the coordination with pyridine may promote the Al–Al bond cleavage. In the next step, the N-coordinated Py molecule dissociates and the [LAl•] radical attacks the 4-position carbon of Py to form the dearomatized intermediate (**INT1**) with a monoanionic radical pyridine bonding to Al^{III} center. The formation of this intermediate is exothermic by 6.8 kcal mol^{-1}. This intermediate then loses the H• to recover the aromaticity of pyridine ring, giving **INT2** [LAl(pyridine-4-yl)] with Al–C bond, which is similar to that reported for the mechanism of formation of magnesium phenyl [(^{Dipp}Nacnac)MgPh·TMEDA] (TMEDA = N,N,N',N'-tetramethylethylenediamine) with loss of H•.[16] Then the **INT2** [LAl(pyridine-4-yl)] fragment hexamerizes to give product **3** through strong N→Al interactions. The occurrence of such radical processes is further proved by experiment, where addition of the radical trapping agent TEMPO led to interruption of the formation of product **3**.

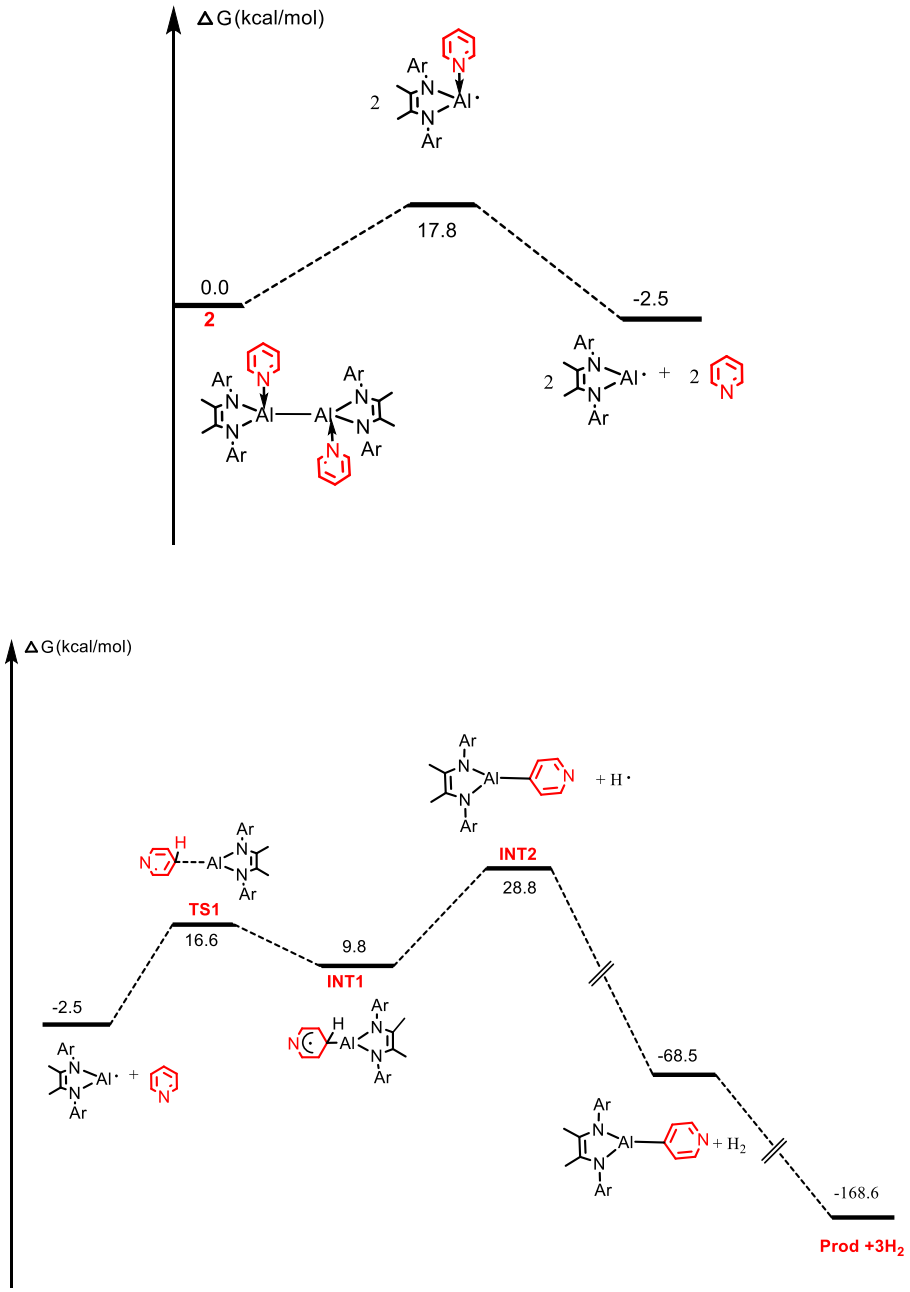

Fig. S19. Energy profile (kcal/mol) for the formation of product **3**.

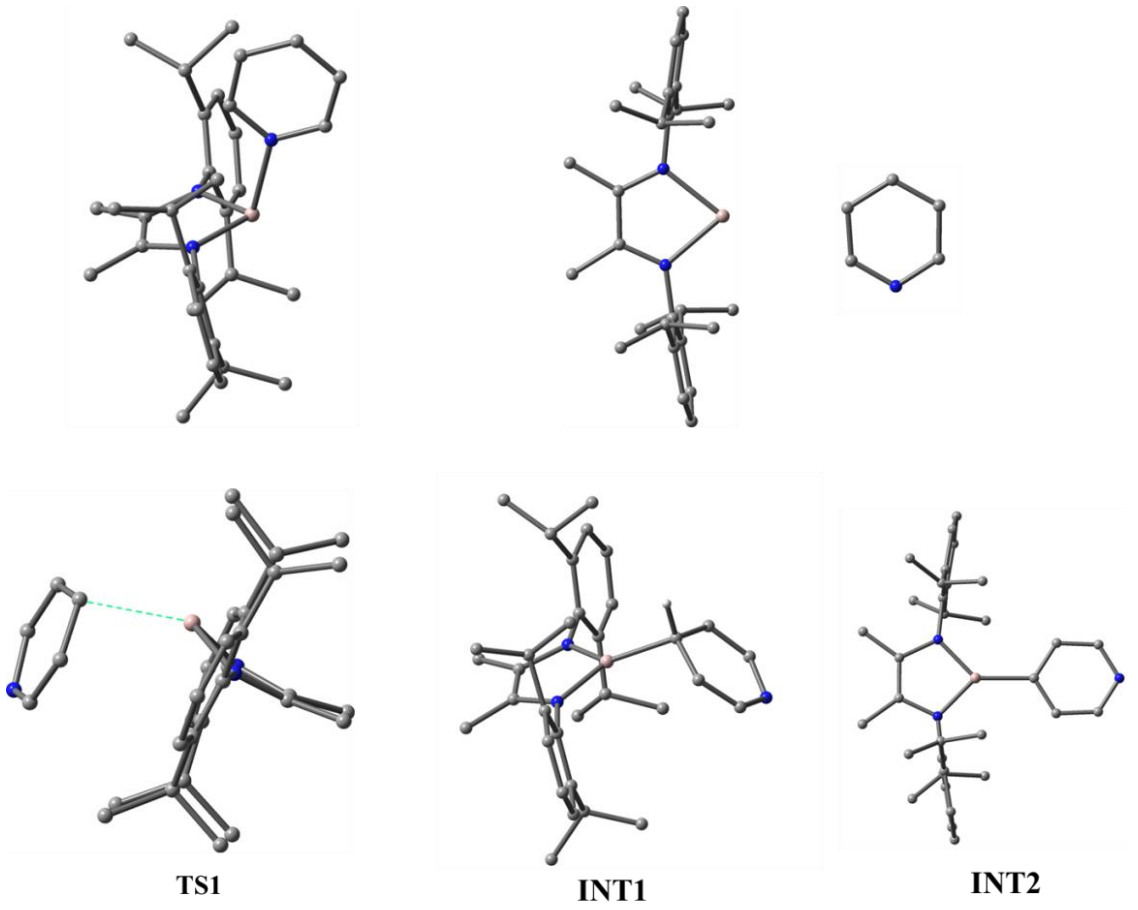

Fig. S20. Optimized structures of intermediate and transition states.

S4. References

(1) H. A. Zhong, J. A. Labinger and J. E. Bercaw, *J. Am. Chem. Soc.*, 2002, **124**, 1378.

(2) Y. Zhao, Y. Liu, L. Yang, J. G. Yu, S. Li, B. Wu and X. J. Yang, *Chem. Eur. J.*, 2012, **18**, 6022.

(3) M. Holz, X. a. Mao, D. Seiferling, A. Sacco, *J. Chem. Phys.*, 1996, **104**, 669.

(4) Sheldrick, G. M. Program SADABS: Area-Detector Absorption Correction, **1996**, University of Göttingen, Germany.

(5) G. M. Sheldrick, *Acta Crystallogr., Sect. C: Cryst. Struct. Commun.*, 2015, **71**, 3.

(6) O. V. Dolomanov, L. J. Bourhis, R. J. Gildea, J. A. K. Howard and H. Puschmann, *J. Appl. Cryst.*, 2009, **42**, 339.

(7) A. L. Spek, *Acta Cryst.*, 2015, C71, 9.

(8) A. D. Becke, *J. Chem. Phys.*, 1993, **98**, 5648.

(9) C. Lee, W. Yang and R. G. Parr, *Phys. Rev. B.*, 1988, **37**, 785.

(10) Gaussian 09, Revision C.1, M. J. Frisch, G. W. Trucks, H. B. Schlegel, G. E. Scuseria, M. A. Robb, J. R. Cheeseman, G. Scalmani, V. Barone, B. Mennucci, G. A. Petersson, H. Nakatsuji, M. Caricato, X. Li,

H. P. Hratchian, A. F. Izmaylov, J. Bloino, G. Zheng, J. L. Sonnenberg, M. Hada, M. Ehara,; K. Toyota, R. Fukuda, J. Hasegawa, M. Ishida, T. Nakajima, Y. Honda, O. Kitao, H. Nakai, T. Vreven, Jr., J. A. Montgomery, J. E. Peralta, F. Ogliaro, M. Bearpark, J. J. Heyd, E. Brothers, K. N. Kudin, V. N. Staroverov, R. Kobayashi, J. Normand, K. Raghavachari, A. Rendell, J. C. Burant, S. S. Iyengar, J. Tomasi, M. Cossi, N. Rega, J. M. Millam, M. Klene, J. E. Knox, J. B. Cross, V. Bakken, C. Adamo, J. Jaramillo, R. Gomperts, R. E. Stratmann, O. Yazyev, A. J. Austin, R. Cammi, C. Pomelli, J. W. Ochterski, R. L. Martin, K. Morokuma, V. G. Zakrzewski, G. A. Voth, P. Salvador, J. J. Dannenberg, S. Dapprich, A. D. Daniels, Ö. Farkas, J. B. Foresman, J. V. Ortiz, J. Cioslowski and D. J. Fox, Gaussian, Inc., Wallingford CT, 2009.

(11) O. V. Sizova, L. V. Skripnikov and A. Y. Sokolov, *J. Mol. Struct.: THEOCHEM*, 2008, **870**, 1–9.

(12) A. E. Reed, L. A. Curtiss and F. Weinhold, *Chem. Rev.* 1988, **88**, 899.

(13) K. B. Wiberg, *Tetrahedron*, 1968, **24**, 1083.

(14) C. Jones, D. D. L. Jones, I. Douair, L. Maron, A*ngew. Chem. Int. Ed.*, DOI: doi.org/10.1002/anie.202017126.

(15) G. Wang, H. Zhang, J. Zhao, W. Li, J. Cao, C. Zhu, S. Li, *Angew. Chem. Int. Ed.* 2016, **55**, 5985.

(16) T. X. Gentner, B. Rösch, G. Ballmann, J. Langer, H. Elsen and S. Harder, *Angew. Chem. Int. Ed.* 2019, **58**, 607.